AIAA JOURNAL
Vol. 45, No. 2, February 2007

# Vortex Lock-In Phenomenon in the Wake of a Plunging Airfoil

John Young* and Joseph C. S. Lai†
*University of New South Wales, Australian Defence Force Academy, Canberra, Australian Capital Territory 2600, Australia*

DOI: 10.2514/1.23594

**The flow over a NACA0012 airfoil, oscillated sinusoidally in plunge, is simulated numerically using a two-dimensional Navier–Stokes solver at a Reynolds number of 20,000. The wake of the airfoil is visualized using a numerical particle tracing method for high reduced frequencies ($1.0 < k < 10.0$) and small nondimensional amplitudes ($h < 0.1$). Anomalous vortex shedding modes (involving multiple vortices shed per half-cycle of airfoil motion) observed experimentally in the literature are reproduced numerically and are shown to be the result of interaction between the plunging frequency and a natural bluff-body shedding frequency. This results in a vortex lock-in phenomenon analogous to that seen for oscillating cylinders. However, the lock-in boundary is not symmetric about the natural shedding frequency, due to the sharp trailing edge forcing the flow to separate at the trailing edge on the windward side of the airfoil for the majority of the plunge cycle at higher frequencies and amplitudes.**

## Nomenclature

| | | |
|---|---|---|
| $c$ | = | airfoil chord |
| $f$ | = | plunge frequency |
| $h$ | = | plunge amplitude nondimensionalized by airfoil chord |
| $k$ | = | reduced frequency $\pi fc/U_\infty$ |
| $k_{\text{nat}}$ | = | reduced natural shedding frequency |
| $Re$ | = | freestream Reynolds number |
| $t$ | = | time |
| $\tau$ | = | nondimensional time $t/T$ |
| $T$ | = | plunge motion period $f^{-1}$ |
| $U_\infty$ | = | freestream velocity |

## I. Introduction

EARLY theoretical analyses by Theodorsen [1] and Garrick [2] and a number of experimental and computational studies (e.g., Katzmayr [3], Koochesfahani [4], and Dohring et al. [5]) have shown that oscillating airfoils generate thrust at certain combinations of oscillation frequency and amplitude. Freymuth [6], Koochesfahani [4], Jones et al. [7], and Lai and Platzer [8] showed through experiments that the wakes of oscillating airfoils can be characterized as drag-producing, neutral, or thrust-producing depending on the frequency and amplitude. Such wakes are typically characterized by rows of vortices shed from the airfoil as the bound circulation changes throughout the flapping cycle. Drag-producing wakes exhibit a classic Kármán vortex street (with a momentum deficit in the time-averaged flow); thrust-producing wakes transpose the vortex rows in a so-called reverse Kármán vortex street (with a momentum excess, or jet, in the time-averaged flow); in neutral wakes the vorticity is shed approximately along the centerline of the oscillation. However, Lai and Platzer [8] found experimentally that for a plunging NACA0012 airfoil (using a rectangular planform wing of aspect ratio 3.7 to create a nominally 2-D flow) at Reynolds number $Re = 20,000$, for a reduced frequency range of $0 < k < 8$ and an amplitude range of $0 < h < 0.1$, the wake formations did not smoothly change from Kármán to neutral to reverse Kármán vortex streets as the plunge amplitude and the thrust of the airfoil were increased. Rather, there were a number of transitional forms for which multiple vortices were shed from the trailing edge per half-cycle of airfoil motion. These wake formations appeared for low drag or approximately zero net thrust and were sensitive to the plunging frequency. This behavior was replicated numerically with very good agreement by Young and Lai [9], using a 2-D Navier–Stokes solver.

A detailed understanding of the wakes shed by oscillating airfoils is important to the study of flutter in aircraft wings, helicopter rotor blades, and turbomachinery blades. The frequency and amplitude of velocity and pressure fluctuations in the wake and the aeroelastic behavior of the wing or blade are directly linked. In the case of helicopters and turbomachinery, the wake of a foregoing blade can also have a strong effect on following blades, due to impingement of the vortical structures. Similarly, the strength and arrangement of the wake structures generated by the airfoil will determine the noise signature generated in the far field in an aeroacoustic context. Gostelow et al. [10] pointed out the similarities between oscillating cylinder (bluff body) and oscillating airfoil (streamlined, with a sharp trailing edge) flows and the vortex shedding created by an oscillating flowfield over a stationary airfoil in a transonic turbine cascade. The current work considers the small-amplitude, high-frequency motions associated with aeroelastic and aeroacoustic phenomena, to provide an explanation for some of the observed wake structures. Large-amplitude, low-frequency motions more relevant to biohydrodynamics (such as fish and cetacean propulsion, as well as bird, insect, and micro air vehicle aerodynamics) are considered elsewhere [11–13].

## II. Numerical Method

The unsteady flowfield around an oscillating airfoil is simulated using a second-order-accurate 2-D compressible Navier–Stokes (NS) solver at low Mach number ($M_\infty = 0.05$). The equations are solved on a structured C-grid wrapped around the airfoil. The method uses Crank–Nicolson second-order time discretization; viscous flux terms are evaluated using second-order central differences in space, and inviscid fluxes are evaluated with a third-order-accurate Osher upwind scheme. The resulting semi-implicit equations are solved using Newton subiteration. Motion of the airfoil is introduced by a combination of rigid-body motion and deformation of the grid. A numerical particle tracing method is implemented to bring out small details of the wake structures. Details of the method and quantitative and qualitative validation against results in the literature may be found in Young [13], Young and Lai [9], and Tuncer and Platzer

Received 3 March 2006; revision received 13 July 2006; accepted for publication 12 November 2006. 

*Lecturer, School of Aerospace, Civil and Mechanical Engineering; j.young@adfa.edu.au. Member AIAA.
†Professor, School of Aerospace, Civil and Mechanical Engineering; j.lai@adfa.edu.au. Associate Fellow AIAA.

[14]. Results presented here use a $1081 \times 121$ grid (377 points around the airfoil surface, first normal grid point at $9.2 \times 10^{-5}$ chord lengths from the surface), boundaries at 20 chords from the airfoil, and nondimensional time step $\Delta\tau = 7.5 \times 10^{-6}$ (for $k = 1.0$) to $7.5 \times 10^{-5}$ (for $k = 10.0$), for which the wake structures are independent of the grid and time step. The flow is assumed to be fully laminar [9] at Reynolds number $Re = 20,000$.

To isolate and compare elements of the controlling physics of the plunging airfoil flow, an unsteady panel method (UPM) code has also been developed [9,13], following Basu and Hancock [15] and Jones et al. [16]. The method assumes inviscid and incompressible flow, enforces the Kutta condition at the trailing edge, and does not allow any separation over the airfoil surface. As the airfoil translates and the lift changes, vorticity is shed into the wake at each time step and is allowed to evolve according to self-induced velocities, thus the nonlinear character of the wake is preserved. Validation of the method was given by Young [13]. Results presented here use 400 panels around the airfoil and 200 Rankine vortices shed into the wake, per flapping cycle.

## III. Multiple Vortex Pair Shedding Modes and Vortex Lock-In

Figure 1 shows the wake structure behind a plunging airfoil for $k = 4.0$, $h = 0.0125$, and $Re = 20,000$. Under these conditions, the wake displays multiple vortices shed from the trailing edge per half-cycle of airfoil motion, as seen in the experimental dye visualization of Lai and Platzer [8] (top frame). The wake structure is well reproduced by the Navier–Stokes solver (middle frame), but the panel method code produces a qualitatively different wake, showing only a single vortex shed per half-cycle (bottom frame). The panel method does not account for viscosity and prevents any separation on the airfoil surface, indicating that the source of the multiple-vortex-per-half-cycle shedding mechanism is a viscous effect rather than due to wake evolution, which is essentially an inviscid phenomenon.

The multiple-vortex-per-half-cycle shedding apparent in Fig. 1 is not due to leading-edge shedding and interaction of leading and trailing-edge vortices. This may be seen by referring to Fig. 2, which shows the vorticity distribution around the entire airfoil as predicted by the Navier–Stokes solver for $k = 4.0$, $h = 0.0125$, and $Re = 20,000$; there is no evidence of any leading-edge vortices under these conditions. The wake structure must then be a result of vorticity shedding into the wake at, or close to, the trailing edge.

At $Re = 20,000$, the stationary airfoil, even though streamlined, acts somewhat like a bluff body. The flow separates upstream of the trailing edge on both sides of the airfoil, creating an effectively blunt-edged body around which the remainder of the fluid flows. Vortices are shed alternately from either side of the trailing edge in a manner

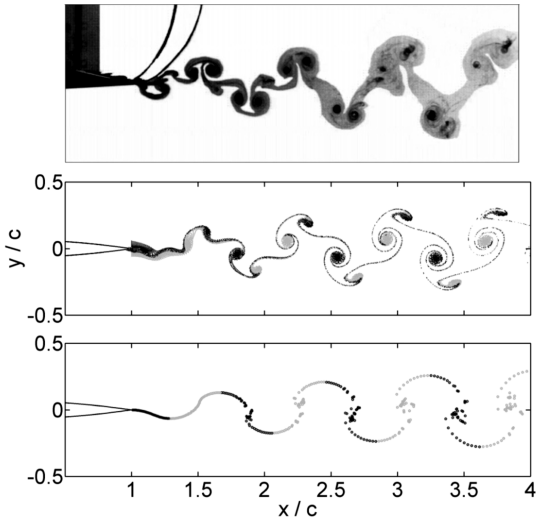


**Fig. 1 Comparison of experimental (top, Lai and Platzer [8]), Navier–Stokes (middle), and panel method (bottom) wake visualizations; $k = 4.0$, $h = 0.0125$, and $Re = 20,000$.**

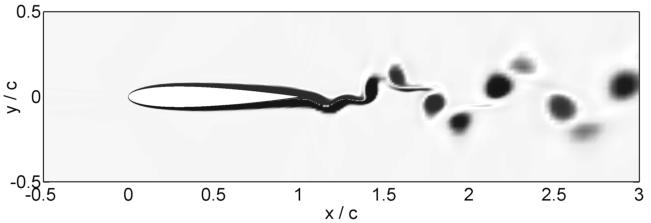


**Fig. 2 Vorticity contours, Navier–Stokes simulation; $k = 4.0$, $h = 0.0125$, and $Re = 20,000$.**

analogous to the shedding behind a circular cylinder, as shown in Fig. 3. The separation regions on either side of the trailing edge persist for the plunging airfoil, and the degree of effective bluntness of the airfoil trailing edge varies throughout the plunge cycle, as well as with $k$ and $h$. The trailing edge of the airfoil, now acting as a bluff body, will have a vortex shedding frequency associated with it that will vary somewhat with the Reynolds number. This shedding mode is hereafter referred to as *natural shedding*, as opposed to the *forced shedding* induced by the motion of the airfoil. For validation, the Navier–Stokes simulation produced a natural shedding frequency of approximately $k_{\text{nat}} = 8.5$ for $Re = 12,000$, as determined by measurement of the maximum power spectral density of the vertical velocity in the wake 1.5 chords aft of the trailing edge, compared with the experimental value of 8.7 of Koochesfahani [4]. For $Re = 20,000$, the natural shedding frequency was $k_{\text{nat}} = 9.4$. The presence of a natural shedding frequency due to trailing-edge separation for the airfoil in the Reynolds number range under investigation, in addition to the forced frequency imposed by the airfoil motion, leads to the possibility of interaction between the two frequencies.

Such interaction between natural shedding and forced frequencies is well known in the vibration of circular cylinders and other bluff bodies. Karniadakis and Triantafyllou [17] studied the wake of a cylinder in laminar flow using a spectral elements Navier–Stokes solver. They noted the experimental results of Koopman [18], showing that below a certain amplitude of forced transverse vibration, only the natural shedding frequency is apparent in the wake of the cylinder. Above the threshold-forcing amplitude, the forcing frequency becomes visible in the wake structures.

Karniadakis and Triantafyllou [17] used a numerical forcing function in the wake, consisting of a local additional acceleration, to simulate the effect of an active control device such as a thin vibrating wire. They showed that on a graph of forcing amplitude versus forcing frequency, the wake can select one of three possible states. Inside a roughly parabolic region of the graph centered on the natural shedding frequency and above a threshold amplitude, the wake oscillates periodically at the forced frequency. This is known as the vortex *lock-in region*, and the boundary is known as the *lock-in boundary*. Outside this region, there is a *receptivity boundary*, inside which there is interaction between the forced and natural frequencies leading to quasi-periodic and nonperiod (chaotic) vortex shedding. Outside the receptivity boundary, the wake oscillates periodically at the natural shedding frequency.

Patnaik et al. [19] examined the laminar flow past a transversely vibrating cylinder using a finite element Navier–Stokes solver. Here,

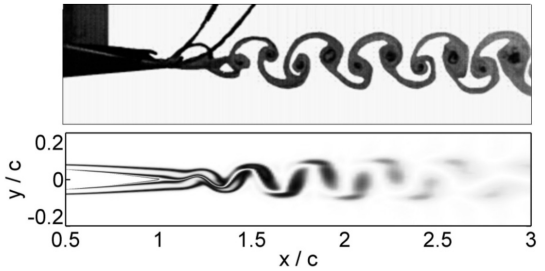


**Fig. 3 Experimental (top, Lai and Platzer [8]) and Navier–Stokes (bottom, vorticity contours) wake visualizations, stationary airfoil; $Re = 20,000$.**

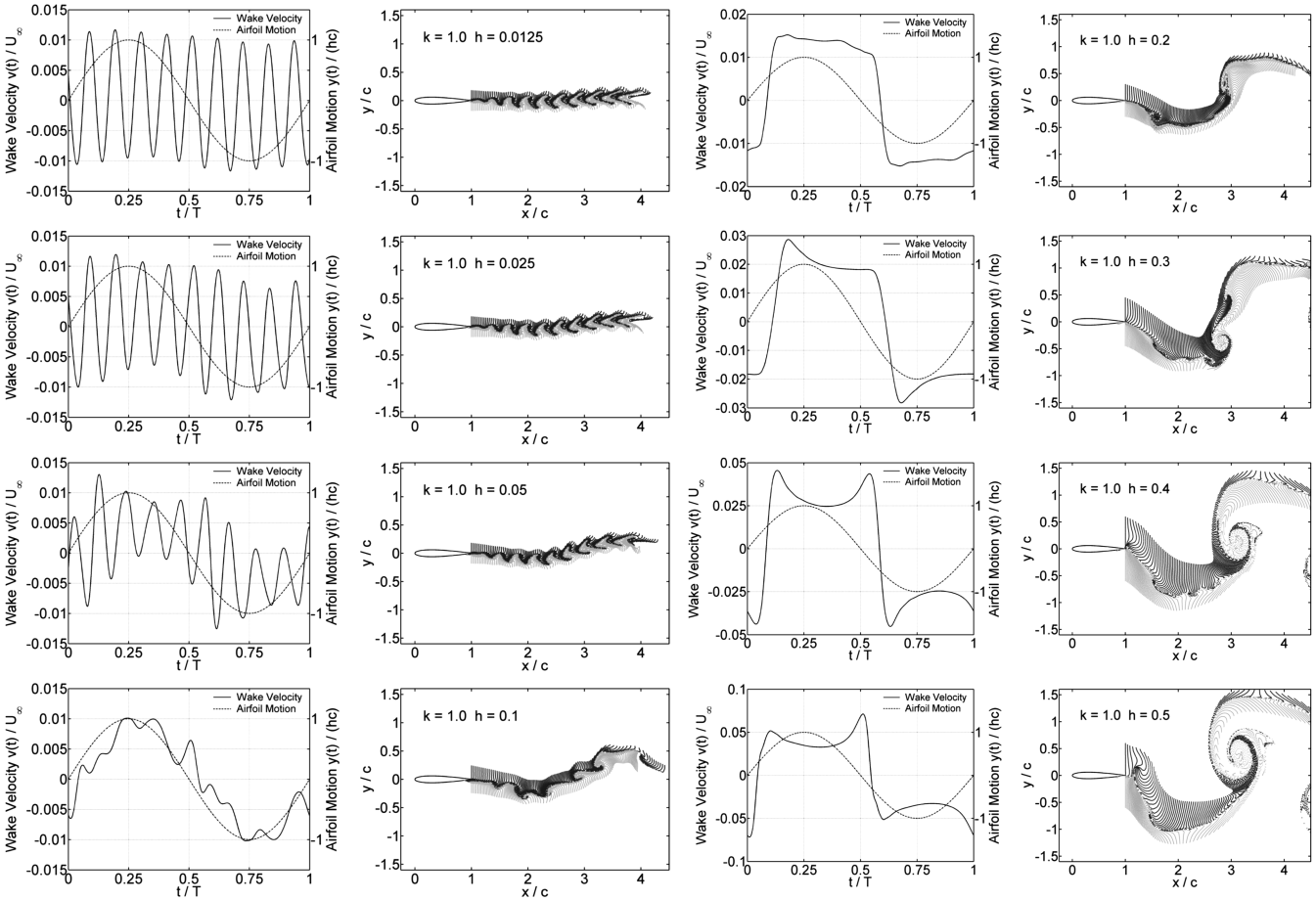


**Fig. 4 Navier–Stokes vertical velocity time history in the wake (left) and wake particle traces (right), showing the onset of vortex lock-in with increasing plunge amplitude $h$, for $k = 1.0$ and $Re = 20,000$. Velocity measured at the fixed location in the wake $x/c = 1.5$ and $y/c = 0.0$.**

the forcing was due to the motion of the cylinder, rather than any control device in the wake. They calculated an approximate lock-in boundary and found it to be roughly of the shape stated in Karniadakis and Triantafyllou [17] and as found by other researchers.

It is reasonable to expect that a similar phenomenon may manifest itself in the wake of the plunging airfoil, although the different geometry may give rise to a different lock-in boundary shape. This possibility is investigated next.

Figure 4 shows a series of particle traces (right frames) generated with reduced frequency held constant at $k = 1.0$, and plunge amplitude $h$ varied from 0.0125 to 0.5. The left frames show the vertical velocity measured in the wake throughout the plunging cycle, at a fixed point in the wake on the centerline of the motion, half a chord length downstream of the trailing edge. The natural shedding frequency is apparent in the first three particle traces ($h = 0.0125$ to 0.05) and remains at $k_{\text{nat}} = 9.4$, measured as described previously. The corresponding velocity time histories are dominated by the natural shedding. Note that the shedding frequency is not an integral multiple of the plunging frequency, and so the velocity time histories do not have equal values at the beginning and end of the flapping cycle. Multiple vortices are shed per half-cycle of airfoil motion, but the shedding is uncorrelated with the motion.

For $k = 1.0$ and $h = 0.1$, the particle trace shows a qualitatively different shedding behavior in comparison with the smaller amplitudes. The velocity time history has become periodic at $h = 0.1$. Thus, the superimposed natural shedding frequency has now changed to a harmonic of the flapping frequency, and the multiple-vortex-per-half-cycle shedding is correlated with the airfoil motion.

As the plunge amplitude $h$ is increased further, an integer number of vortices is shed per half-cycle, and the number of vortices appears to decrease with increasing $h$. The wake velocity measurements show that as $h$ is increased, the dominant frequency in the wake is initially the natural shedding frequency ($k_{\text{nat}} = 9.4$), but at a certain critical amplitude threshold (approximately $h = 0.1$ for $k = 1.0$), the plunging (forcing) frequency becomes dominant. For the highest amplitudes ($h = 0.4$–$0.5$), there appear to be a number of small Helmholtz vortices in the shear layer immediately aft of the trailing edge, but these are quickly wrapped up into a single large vortex per half-cycle in the wake.

A similar pattern is observed at higher reduced frequencies. Figures 5 and 6 show wake particle traces for $k = 5.0$ and $k = 10.0$, respectively. For $k = 5.0$, as for $k = 1.0$, the forcing frequency is below the natural shedding frequency at the Reynolds number considered here ($Re = 20,000$). The first frame of Fig. 5 ($h = 0.00125$) shows the wake dominated by natural shedding. At $h = 0.0025$, there is some kind of transition process occurring, and at $h = 0.005$, the wake is dominated by shedding at the forcing frequency.

In Fig. 6, the forcing frequency is now above the natural shedding frequency. For $h = 0.00025$ and $h = 0.0005$, the shedding into the wake is at the natural shedding frequency. At $h = 0.00125$, the dominant shedding mode in the wake has switched to the forcing frequency. This can be seen by counting the number of vortices visible in the wake, although this is a qualitative measure only; as the plunge amplitude is increased further, the airfoil starts to produce thrust instead of drag, and the wake vortices are convected further downstream at the same time, taking some of them out of the view in the frames shown. However, the switchover from natural shedding to forced frequency is quite apparent in the wake particle traces shown for the higher frequencies of $k = 5.0$ and $k = 10.0$.

An approximate vortex lock-in boundary on the $h$–$k$ plane, based on the data in Figs. 4–6, is plotted in Fig. 7. It can be seen that this boundary does not follow a contour of constant $kh$. The plunging frequency is normalized against the natural shedding frequency of

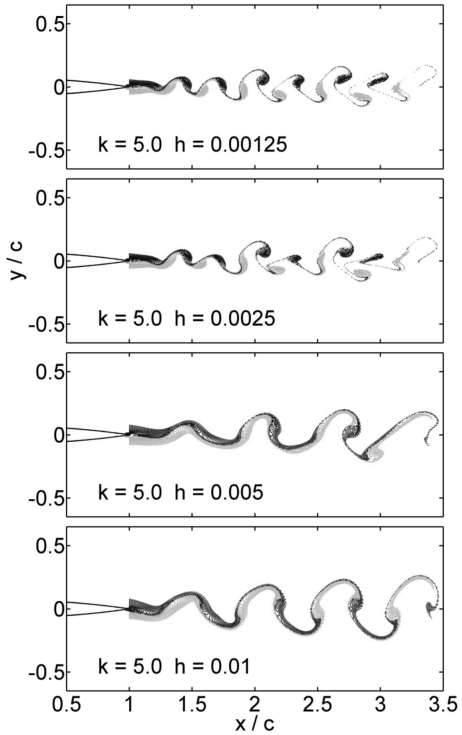


**Fig. 5 Navier–Stokes wake particle traces showing the onset of vortex lock-in with increasing plunge amplitude $h$, for $k = 5.0$ and $Re = 20,000$. Lock-in occurs between $h = 0.0025$ and $h = 0.005$.**

approximately $k_{nat} = 9.4$. The boundary divides the $h$–$k$ plane into regions in which either the natural shedding frequency or the forcing (plunging) frequency dominates the wake.

By analogy with the receptivity boundary of the circular cylinder case, a *harmonic region* is also shown (again, this is approximate only). Inside the harmonic region, the airfoil may display vortex shedding at some higher (integer) harmonic of the forcing frequency.

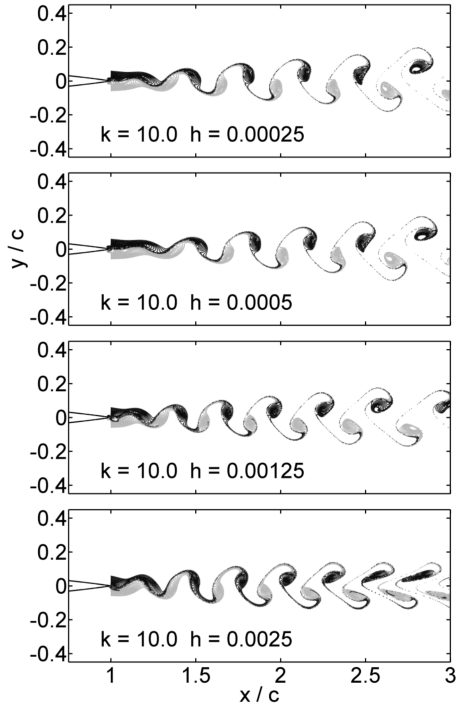


**Fig. 6 Navier–Stokes wake particle traces showing the onset of vortex lock-in with increasing plunge amplitude $h$, for $k = 10.0$ and $Re = 20,000$. Lock-in occurs between $h = 0.0005$ and $h = 0.00125$.**

The harmonic boundary must meet the vortex lock-in boundary at $k/k_{nat} = 0.5$, because above this value, any harmonic of the forcing frequency would be above the natural shedding frequency. This is supported by the wake visualizations of Figs. 4–6. For $k = 1.0$, the wake demonstrates a variety of shedding modes as $h$ is increased, whereas for $k = 5.0$ and $k = 10.0$ (both above $k/k_{nat} = 0.5$), the wake changes quite abruptly from natural shedding to forced shedding with increasing plunge amplitude.

Unlike the circular cylinder case, the vortex lock-in boundary is not likely to be symmetric about the natural shedding frequency. This is due to the sharp trailing edge of the airfoil, which fixes the separation point for values of $k > k_{nat}$ and higher values of $h$, and ensures that the shedding takes place at the forcing frequency (i.e., vortex lock-in). This may be seen in the instantaneous streamlines of Fig. 8, in which, at very low plunge amplitude, the flow separates upstream of the trailing edge on both sides of the airfoil, creating an effectively blunt-ended body, as depicted in Fig. 3. Animations of the flowfield show that the area on the airfoil from which vorticity is shed into the wake alternates between the top and bottom surfaces as the relative sizes of the two separation regions change throughout the plunge cycle and gives rise to the multiple-vortex-per-half-cycle shedding. At higher amplitudes, the flow is forced by the sharp trailing edge to separate at the trailing edge on the windward side of the airfoil for the majority of the half-cycle of airfoil motion, resulting in one large vortex being shed per half-cycle.

Also shown in Fig. 7 are two constant-$kh$ contours, at $kh = 0.05$ and $kh = 0.1$. The data points are for $k$ values of 1.0, 2.0, 4.0, 5.0, and 8.0 in each case. If we follow the $kh = 0.05$ contour from low to high frequency, we observe the following behavior. At $k = 1.0$, the airfoil is in the natural shedding region, and the wake is dominated by the natural shedding frequency, as shown for $k = 1.0$ and $h = 0.05$ in Fig. 9 (note that the frames are normalized against the plunge amplitude (and, hence, the inverse of the frequency, because $kh$ is constant here) to show all the wakes at the same wavelength for easy comparison of the vortex shedding regime). At $k = 2.0$, the airfoil is close to the harmonic region (or perhaps inside, because the boundaries are only drawn approximately), and in Fig. 9, the wake for $k = 2.0$ and $h = 0.025$ shows a slow variation, with more rapid vortex shedding superimposed. At $k = 4.0$, the airfoil is now inside the harmonic region, and the wake for $k = 4.0$ and $h = 0.0125$ shows two vortices being shed per half-cycle (thus, the shedding is taking place at twice the plunging frequency). At $k = 5.0$, the airfoil is now fully inside the vortex lock-in region. This is confirmed by the $k = 5.0$ and $h = 0.01$ frame, in which only the forcing frequency is apparent in the wake particle trace. Finally, for $k = 8.0$ and $h = 0.00625$, the airfoil remains inside the vortex lock-in region and, again, we see only the forcing frequency apparent in the wake.

A similar sequence may be followed for the $kh = 0.1$ contour, with wake visualizations presented in Fig. 10. Figures 9 and 10

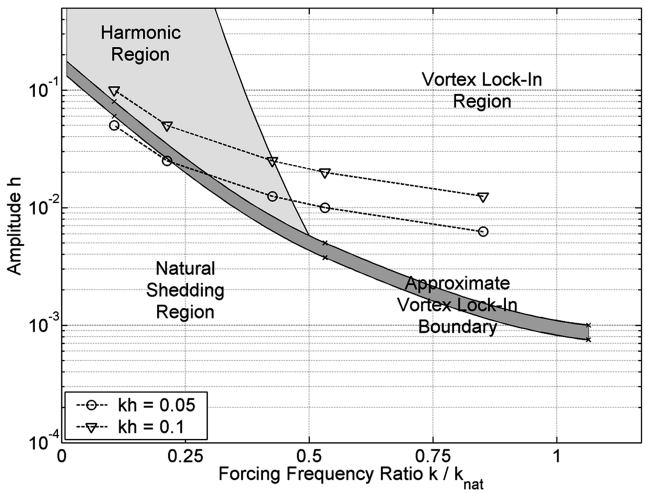


**Fig. 7 Schematic vortex lock-in boundary for a NACA0012 airfoil at $Re = 20,000$.**

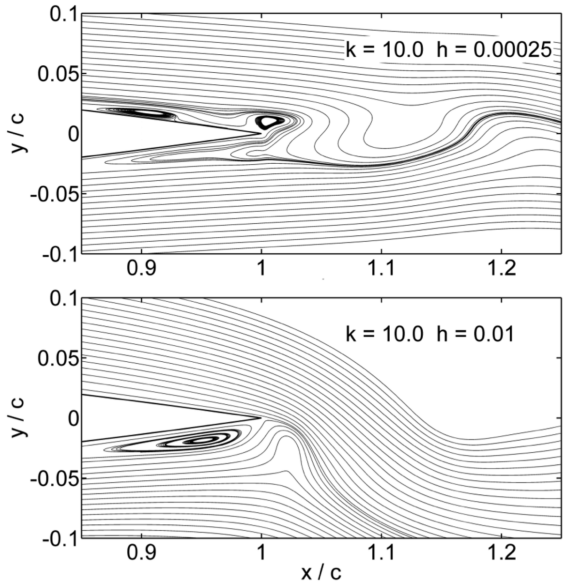


**Fig. 8 Instantaneous streamlines at the trailing edge; airfoil moving upwards through $y = 0$ in both cases.**

illustrate the change from the multiple- to single-vortex-per-half-cycle shedding observed in Lai and Platzer [8] and Young and Lai [9], and Fig. 7 confirms that this behavior is the result of an interaction between the natural shedding frequency of the airfoil at the Reynolds number studied and the forcing frequency $k$. This frequency dependence is expected to diminish with increasing Reynolds number (for which the flow is more likely to be turbulent),

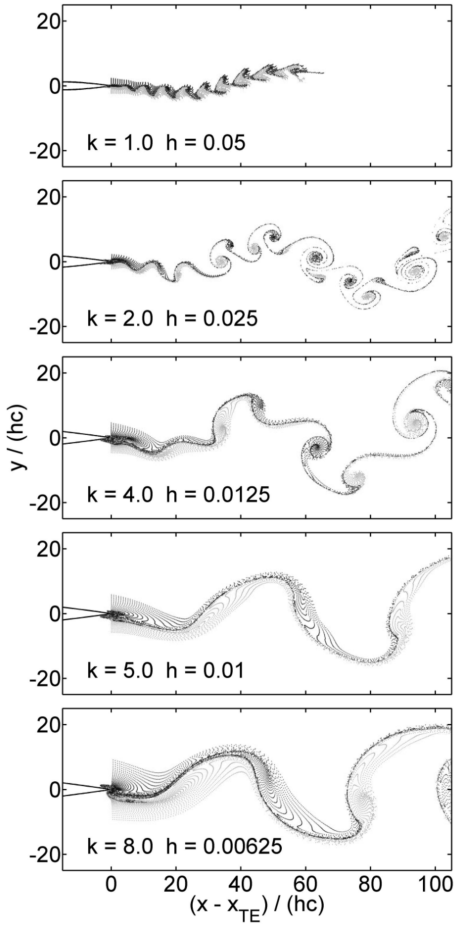


**Fig. 9 Navier–Stokes wake visualizations; $kh = 0.05$, scale normalized against plunging amplitude.**

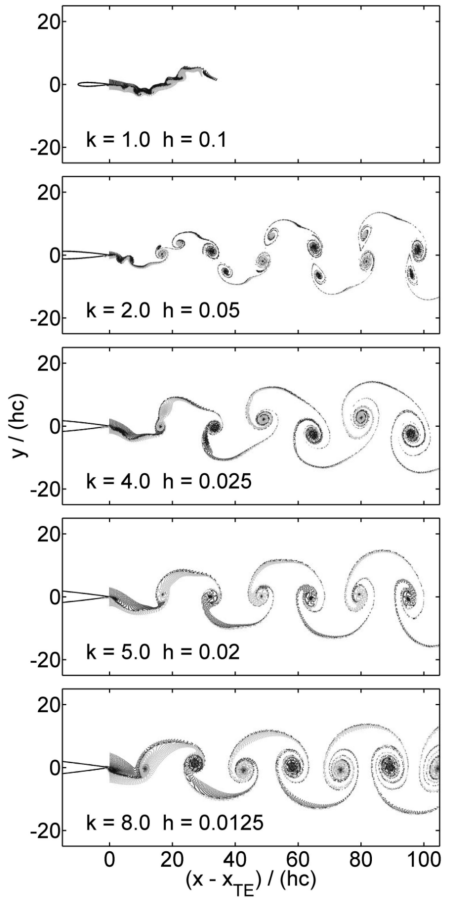


**Fig. 10 Navier–Stokes wake visualizations; $kh = 0.1$, scale normalized against plunging amplitude.**

as evidenced by the large differences between laminar and turbulent simulations at the low flapping amplitudes seen in Young and Lai [9]. Turbulent flow in the boundary layer would decrease the incidence of laminar separation bubbles on the windward side of the airfoil seen in the upper frame of Fig. 8, making the flow look more like the lower frame and bringing the wake closer to a lock-in state. It should also be noted that the observed harmonic (multiple-vortex-per-half-cycle) shedding is not necessarily associated with the change from drag production to thrust production as $h$ is increased for a given $k$. This may be seen in Fig. 5, in which all the wakes show the forward-tilted vortex pairs that are characteristic of drag production.

## IV. Conclusions

The multiple-vortex-per-half-cycle shedding observed by Lai and Platzer [8] was determined to be the result of an interaction between the frequency of bluff-body type natural shedding around the trailing edge and the frequency of the plunging motion of the airfoil. The wake of the airfoil was shown to exhibit vortex lock-in as the amplitude of motion was increased in a manner analogous to that seen for vibrating circular cylinders, although the lock-in boundary was not symmetric about the natural shedding frequency, due to the sharp trailing edge forcing the flow to separate at the trailing edge on the windward side of the airfoil for the majority of the plunge cycle at higher frequencies and amplitudes. As the plunging frequency is increased well above the natural shedding frequency, lock-in is expected to be observed for lower plunge amplitudes, in contrast to the circular cylinder case. At Reynolds number $Re = 20,000$, the wake was shown to be dependent both on reduced frequency $k$ and plunge amplitude $h$ independently, because the natural (bluff-body) shedding had an associated frequency and the vortex lock-in process introduced a flapping frequency dependence into the wake structure of the airfoil. This frequency dependence is expected to diminish

with increases in Reynolds number and the corresponding transition to turbulence in the boundary layer.

## Acknowledgment

This work was supported by an award under the Merit Allocation Scheme on the National Facility of the Australian Partnership for Advanced Computing (APAC).

## References

[1] Theodorsen, T., "General Theory of Aerodynamic Instability and the Mechanism of Flutter," NACA TR-496, 1935.

[2] Garrick, I. E., "Propulsion of a Flapping and Oscillating Airfoil," NACA Report No. 567, 1937.

[3] Katzmayr, R., "Effect of Periodic Changes of Angle of Attack on Behavior of Airfoils," NACA TM-147, 1922.

[4] Koochesfahani, M. M., "Vortical Patterns in the Wake of an Oscillating Airfoil," *AIAA Journal*, Vol. 27, No. 9, 1989, pp. 1200–1205.

[5] Dohring, C. M., Platzer, M. F., Jones, K. D., and Tuncer, I. H., "Computational and Experimental Investigation of the Wakes Shed From Flapping Airfoils and Their Wake Interference/Impingement Characteristics," *The Characterisation and Modification of Wakes from Lifting Vehicles in Fluids*, Vol. 33, AGARD, Neuilly-sur-Seine, France, 1996, pp. 1–9.

[6] Freymuth, P., "Propulsive Vortical Signature of Plunging and Pitching Airfoils," *AIAA Journal*, Vol. 26, No. 7, 1988, pp. 881–883.

[7] Jones, K. D., Dohring, C. M., and Platzer, M. F., "Experimental and Computational Investigation of the Knoller–Betz Effect," *AIAA Journal*, Vol. 36, No. 7, 1998, pp. 1240–1246.

[8] Lai, J. C. S., and Platzer, M. F., "Jet Characteristics of a Plunging Airfoil," *AIAA Journal*, Vol. 37, No. 12, 1999, pp. 1529–1537.

[9] Young, J., and Lai, J. C. S., "Oscillation Frequency and Amplitude Effects on the Wake of a Plunging Airfoil," *AIAA Journal*, Vol. 42, No. 10, 2004, pp. 2042–2052.

[10] Gostelow, J. P., Carscallen, W. E., and Platzer, M. F., "On Vortex Formation in the Wake Flows of Transonic Turbine Blades and Oscillating Airfoils," ASME Turbo Expo 2005, Reno-Tahoe, NV, International Gas Turbine Inst. Paper GT2005-69128, 2005.

[11] Young, J., Lai, J. C. S., Kaya, M., and Tuncer, I. H., "Thrust and Efficiency of Propulsion by Oscillating Foils," *Computational Fluid Dynamics 2004*, edited by C. Groth and D. W. Zingg, Springer–Verlag, New York, 2004, pp. 313–320.

[12] Young, J., and Lai, J. C. S., "Oscillating Foil Propulsion: A Comparison of Navier–Stokes and Inviscid Numerical Methods," *Jets, Wakes and Separated Flows*, edited by T. Shakouchi, F. Durst, and K. Toyoda, Mie Univ. Press, Mie, Japan, 2005, pp. 577–582.

[13] Young, J., "Numerical Simulation of the Unsteady Aerodynamics of Flapping Airfoils," Ph.D. Thesis, School of Aerospace, Civil and Mechanical Engineering, Univ. of New South Wales, Australian Defence Force Academy, Canberra, ACT, Australia, 2005.

[14] Tuncer, I. H., and Platzer, M. F., "Computational Study of Flapping Airfoil Aerodynamics," *Journal of Aircraft*, Vol. 37, No. 3, 2000, pp. 514–520.

[15] Basu, B. C., and Hancock, G. J., "The Unsteady Motion of a Two-Dimensional Aerofoil in Incompressible Inviscid Flow," *Journal of Fluid Mechanics*, Vol. 87, No. 1, 1978, pp. 159–178.

[16] Jones, K. D., Dohring, C. M., and Platzer, M. F., "Wake Structures Behind Plunging Airfoils: A Comparison of Numerical and Experimental Results," AIAA Paper 96-0078, 1996.

[17] Karniadakis, G. E., and Triantafyllou, G. S., "Frequency Selection and Asymptotic States in Laminar Wakes," *Journal of Fluid Mechanics*, Vol. 199, Feb. 1989, pp. 441–469.

[18] Koopman, G. H., "The Vortex Wakes of Vibrating Cylinders at Low Reynolds Numbers," *Journal of Fluid Mechanics*, Vol. 28, May 1967, pp. 501–512.

[19] Patnaik, B. S. V., Narayana, P. A. A., and Seetharamu, K. N., "Numerical Simulation of Laminar Flow Past a Transversely Vibrating Circular Cylinder," *Journal of Sound and Vibration*, Vol. 228, No. 3, 1999, pp. 459–475.

K. Fujii
*Associate Editor*